THE EFFECT OF THE THICKNESS OF A PACKED BED ON THE DYNAMIC AND THERMAL BEHAVIOR OF A SOLAR DRYER

Submited on 17/01/2014 – Accepted on 04/08/2014

Abstract

Drying food in the sun is a safe, easy and economical way to preserve food, especially fruits. Cabinet dryers are the most popular equipment for fruit drying. Because of intermittent nature of solar energy, storage is required for uninterrupted supply in order to match the needs. The main objective of this study is to assess effectiveness of continuous solar dryer integrated with packed bed as thermal storage with natural airflow for drying figs (Ficuscarica). The cabinet dryer were envisaged theoretically (computational fluid dynamics (CFD). The distribution of the velocity and temperature of air within the solar dryer were presented during one day of August and under the climate conditions of Tlemcen (Algeria). The effects of presence of a packed bed on the distribution of velocity and temperature of airflow and on the temperature of figs were analyzed. The results show that the solar dryer design, incorporating a packed bed enhances the capabilities and performance of the solar dryer, through increasing time of drying.

Keywords: *packed bed, storage energy, solar dryer, natural convection.*

S KHALDI [1]
S ABBOUDI [2]
A KORTI [3]

1 Faculty of Technology, University of Abou Bekr Belkaid, Tlemcen, Algeria
2 University of Technology of Belfort-Montbéliard, site of Sévenans, France
3 Laboratory IRTES-M3M, University of Technology of Belfort-Montbéliard, site of Sévenans, France

I. INTRODUCTION

At the majority of African countries, agriculture represents the biggest part of economy. The lack of appropriate preservation and storage system caused considerable losses thus reducing the food supply significantly. Drying is the world's oldest and most common method of food preservation. Traditionally drying of agricultural products was by spreading them on the ground in open sun. Togrul and Pehlivan (2004) [1] present a study about the open-air drying factors for some products: apricots, grapes, peaches, figs and plums. They present also a schematic diagram and mathematical model of the open-air drying unit of the studied experimental curves. They compare their results with 12 different models to find the best fitting curve. Jain and Tiwari (2003) [2], present a sketch of the working principles of open solar drying and a mathematical model which predicts the crop temperature, the moisture removal rate and the equivalent solar temperature. Open air natural sun drying presents some problems making this operation not always suited to large scale production and reduce both of quantity and quality of the final product [3]. To overcome such problems, various types of dryers have been developed, which are generally classified into: direct, indirect and mixed mode systems with natural or forced circulation of the drying air. For more details, see references [4] to [8]. The present work is based on a system studied by Dilip (2007)[9], which is analyzed with a global energy balance approach based on the knowledge of heat and mass transfer coefficients between different components of the system. We propose to analyze the same system more precisely on the basis of a complete approach, based on mass, momentum and energy conservation equations in the solid, fluid and porous mediums.

II. DESCRIPTION OF SOLAR DRYER

This section provides a description of the geometrical configuration of solar dryer. In order to find the most appropriate geometrical shape of cabinet dryer for achieving more uniform distribution of drying air flow inside the dryer, after investigating two different shapes (solar dryer with one inlet at left, solar dryer with two inlets). The physical model is presented in Fig.1. The dryer had capacity to dry 23.5 kg fresh figs. The dryer has total collector area of 1m2. Reflector in a polygonal form with five flat segments of identical size reflects the solar radiation to the horizontal absorber-1 (aluminum) which is facing down. The drying installation is placed above the absorber-1 at a distance of e = 0.04 m. This space is necessary for entering ambient air from the two sides. A packed bed with a porosity of 0.4 is placed before the two drying trays (fig.1). The air heated by the absorber-1 flows into the packed bed and warms up the gravel which causes the decrease of air temperature, and then it flows towards the crops trays. An inclined solar chimney (35°) is placed on top of the dryer to assure the forced air extraction. This chimney is composed of glass cover and absorber-2 (aluminum). A heat storage material (granite) is stuck under absorber-2.The absorber-1 absorbs the solar radiation reflected by the reflector. This heat is transferred by convection to the airflow. The hot air flows towards the crop already placed in trays for drying. In the other side, the absorber-2 absorbs solar irradiation transmitted through the glass cover. A part of this heat is transferred by convection to the airflow in channel creating a difference in temperature between the chimney and the outside, the other part is stored by the granite and used during off-sunshine hours for holding an air flow during the drying process. The dimensions and

materials of the solar dryer are presented in the table 1and 2 respectively.

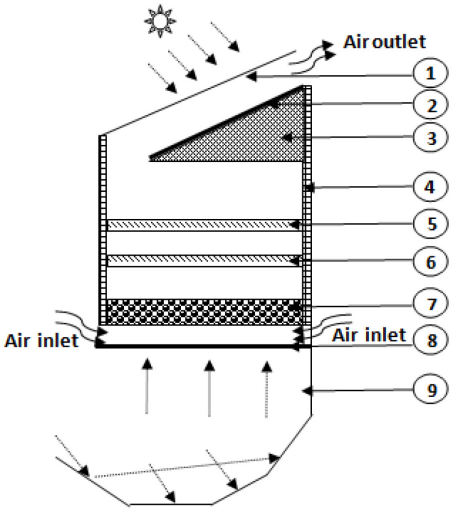

Fig.1: Schematic view of solar dryer (1glass (g), 2 absorber II(p2), 3 storage materiel, 4Wooden wall (w), 5 crop tray II(c2), 6 crop tray I (c1), 7 storage bed (b), 8 absorber I(p1), 9 reflectors).

III. MATHEMATICAL MODELING

A. Assumptions

To simplify the problem, the following assumptions were made:

- The fluid is viscous and newtonien
- The flow is turbulent, two dimensional and unsteady
- The Boussinesq approximation is applied for the buoyancy.
- The thermophysical properties of the air and solids are considered constants.
- The packed bed is homogeneous porous media.

B. Basic governing equations for designing the solar dryer

This model is based on the conservation equations of fluid mechanics: the continuity, the momentum and the energy equations, also it takes into account the turbulent behavior. The general transport equations that describe the principle of conservation of mass, momentum and energy can be expressed in the following conservative form:

- Continuity equation

$$\frac{\partial \rho}{\partial t} + \frac{\partial(\rho u)}{\partial x} + \frac{\partial(\rho v)}{\partial y} = 0 \qquad (1)$$

- Momentum equation

$$\frac{\partial(\rho u)}{\partial t} + \frac{\partial(\rho u u)}{\partial x} + \frac{\partial(\rho v u)}{\partial y} = \frac{\partial}{\partial x}\left(\mu_t \frac{\partial u}{\partial x}\right) + \frac{\partial}{\partial y}\left(\mu_t \frac{\partial u}{\partial y}\right) + S_u \quad (2)$$

$$\frac{\partial(\rho v)}{\partial t} + \frac{\partial(\rho u v)}{\partial x} + \frac{\partial(\rho v v)}{\partial y} = \frac{\partial}{\partial x}\left(\mu_t \frac{\partial v}{\partial x}\right) + \frac{\partial}{\partial y}\left(\mu_t \frac{\partial u}{\partial y}\right) + S_v \quad (3)$$

The source terms in momentum equation:

$$S_u = -\frac{\partial p}{\partial x} + \frac{\partial}{\partial x}\left(\mu_t \frac{\partial u}{\partial x}\right) + \frac{\partial}{\partial y}\left(\mu_t \frac{\partial v}{\partial y}\right) \qquad (4)$$

$$S_v = -\frac{\partial p}{\partial y} + \frac{\partial}{\partial x}\left(\mu_t \frac{\partial u}{\partial y}\right) + \frac{\partial}{\partial y}\left(\mu_t \frac{\partial v}{\partial y}\right) + \rho g \beta (T - T_{ref}) \quad (5)$$

- Energy equation

$$\frac{\partial(\rho T)}{\partial y} + \frac{\partial(\rho u T)}{\partial x} + \frac{\partial(\rho u T)}{\partial y} = \frac{1}{\rho}\left(\frac{\mu}{Pr} + \frac{\mu_t}{\sigma_t}\right)\left(\frac{\partial^2 T}{\partial x^2} + \frac{\partial^2 T}{\partial y^2}\right) \qquad (6)$$

Turbulence kinetic energy k equation:

$$\rho\left(\frac{\partial k}{\partial t} + \frac{\partial(ku)}{\partial x} + \frac{\partial(kv)}{\partial y}\right) = \left(\mu + \frac{\mu_t}{\sigma_k}\right)\left(\frac{\partial^2 k}{\partial x^2} + \frac{\partial^2 k}{\partial x^2}\right) + \rho G_k - \rho\varepsilon \qquad (7)$$

Dissipation rate of turbulent kinetic ε equation:

$$\rho\left(\frac{\partial \varepsilon}{\partial t} + \frac{\partial(\varepsilon u)}{\partial x} + \frac{\partial(\varepsilon v)}{\partial y}\right) = \left(\mu + \frac{\mu_t}{\sigma_\varepsilon}\right)\left(\frac{\partial^2 \varepsilon}{\partial x^2} + \frac{\partial^2 \varepsilon}{\partial x^2}\right) + \frac{\varepsilon}{k}(c_1 \rho G_k - c_2 \rho\varepsilon) \qquad (8)$$

$$\mu_t = \frac{\rho c_\mu k^2}{\varepsilon};\ G_k = \frac{\mu_t}{\rho}\frac{\partial u_i}{\partial x_j}\left\{\frac{\partial u_i}{\partial x_j} + \frac{\partial u_i}{\partial x_i}\right\} \qquad (9)$$

The turbulence model contains five constant which were assigned the following values: $c_\mu = 0.09$, $c_1 = 1.44$, $c_2 = 1.92$, $\sigma_k = 1$, $\sigma_\varepsilon = 1.3$; $\sigma_t = 1$

C. Modeling of the porous bed

The flow in the porous medium is governed by the model of Brinkman-Forchheimer Extended Darcy:

- Continuity equation

$$\frac{\partial \rho}{\partial t} + \frac{\partial(\rho u_f)}{\partial x} + \frac{\partial(\rho v_f)}{\partial y} = 0 \qquad (10)$$

- Momentum equation

$$\frac{\rho}{\epsilon}\frac{\partial u_f}{\partial t} + \frac{\rho}{\epsilon^2}\left(u_f \frac{\partial u_f}{\partial x} + v_f \frac{\partial u_f}{\partial y}\right) = -\frac{\partial p}{\partial x} + \frac{\partial}{\partial x}\left(\mu_{eff}\frac{\partial u_f}{\partial x}\right) + \frac{\partial}{\partial y}\left(\mu_{eff}\frac{\partial u_f}{\partial y}\right) - \mu\frac{u_f}{\theta} + \frac{\rho C\epsilon}{\sqrt{\theta}}|\vec{u_f}|u_f \qquad (11)$$

$$\frac{\rho}{\epsilon}\frac{\partial v_f}{\partial t} + \frac{\rho}{\epsilon^2}\left(u_f \frac{\partial v_f}{\partial x} + v_f \frac{\partial v_f}{\partial y}\right) = -\frac{\partial p}{\partial x} + \frac{\partial}{\partial x}\left(\mu_{eff}\frac{\partial v_f}{\partial x}\right) + \frac{\partial}{\partial y}\left(\mu_{eff}\frac{\partial v_f}{\partial y}\right) - \mu\frac{v_f}{\theta} + \frac{\rho C\epsilon}{\sqrt{\theta}}|\vec{v_f}|v_f + \rho g\beta(T - T_{ref}) \qquad (12)$$

- Energy equation

$$(\rho c)_m \frac{\partial T}{\partial t} + (\rho c)_m\left(u_f \frac{\partial T}{\partial x} + v_f \frac{\partial T}{\partial y}\right) = K_m \frac{\partial}{\partial x}\left(\frac{\partial T}{\partial x}\right) + K_m \frac{\partial}{\partial y}\left(\frac{\partial T}{\partial y}\right) \qquad (13)$$

$$(\rho c)_m = \epsilon(\rho c)_f + (1-\epsilon)(\rho c)_s;\ K_m = \epsilon K_f + (1-\epsilon)K_s \qquad (14)$$

$$\theta = \frac{D_p^2 \epsilon^3}{150(1-\epsilon)^2};\ C = \frac{3.5}{D_p}\frac{(1-\epsilon)}{\epsilon^3}$$

θ is the permeability and C is the inertial resistance factor.

D. Modeling of the crops tray

Fruit trays were assumed as porous media for airflow. It is modeled by the addition of a momentum source term (S_i) to the standard fluid flow equations:

$$S_i = -C_0'|v|^{C_1'} \quad (15)$$

The coefficients C_0' ,C_1' and porosity are proposed for figs fruit by Amanlou and Zomorodian (2010)[10], Porosity of figs bed was measured to be 50.61% and the coefficients C_0' and C_1' were also calculated to be 0.029 and 0.6849, respectively.

E. Initial and boundary conditions

Numerical simulations were performed for a typical day of August, under the climatic conditions of Tlemcen, Algeria. The average global solar intensity G_{sun} and outside air temperature T_a measured are given by Eq. (16) and (17), and presented in Fig. 2.

The outside temperature and the solar irradiance variation are approximated by Eqs. (16) and (17) respectively.

$$T_a(t) = 27 + 7\cos\left(\frac{\pi}{11}(t-15.5)\right) \quad (16)$$

$$G_{sun}(t) = 1068\, sin\left(\pi\frac{t-7}{11}\right);\ 6 < t < 19 \quad (17)$$

The dryer is only heated by direct sunlight from 6 AM to 7 PM.

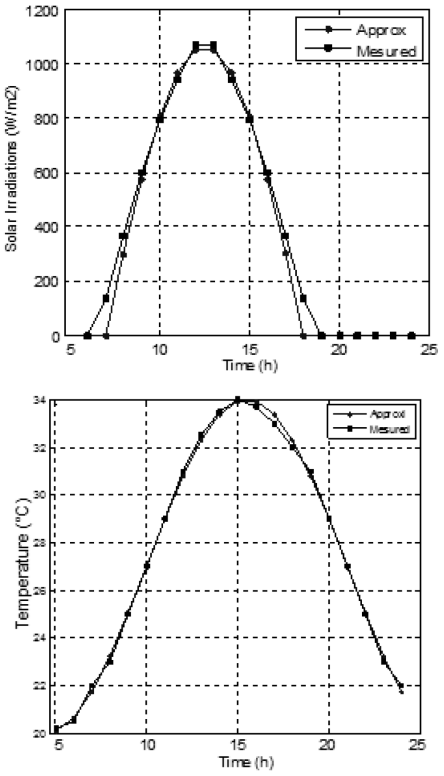

Fig. 2. Average global solar intensity and ambient temperature.

The fluid in the solar dryer is initially stagnant and at a uniform temperature which is the same as the ambient temperature.

The wooden walls surfaces:

$$-K_w\frac{dT}{dn} = h_0(T_w - T_a),\ u=0,\ v=0 \quad (18)$$

Heat transfer coefficient is given by Watmuff et al. (1977)[11]

$$h_0 = 2.8 + 3V_v;\ \ 0 \le V_v \le 7\ m/s \quad (19)$$

The glass surface:

$$-K_g\frac{dT}{dn} = \alpha_g G_{sun}(t) + h_0\left(T_g - T_a\right) + \varepsilon_g\sigma\left({T_g}^4 - T_{sky}^4\right),$$

u=0, v=0 (20)

The sky temperature is given by, Swinbank (1963)[12]

$$T_{Sky} = 0{,}0552\, T_a^{1.5} \quad (21)$$

The solar absorber surface-1:

$$-K_{a1}\frac{dT}{dy} = G_{sun}(t).\rho'.A_t.\alpha_{a1} + h_0(T_{a1} - T_a) \quad (22)$$

u=0, v=0

The solar absorber surface-2:

$$-K_{a2}\frac{dT}{dn} = G_{sun}(t).\tau_g.\alpha_{a2},\ u=0,\ v=0 \quad (23)$$

The inlet of drying system: $T_{inlet} = Ta, p_{inlet} = 10^5 pa$

Outlet of the dryer: $p_{outlet} = 10^5 pa$

Porous media:

- For the bed: $\theta = 6.29\ 10^{-7}$ m^2, C=1719.4 m^{-1}.
- For the trays: C_0'= 0.029, C_1' = 0.6849.

Initial conditions: t=0 $\begin{cases} u = v = 0 \\ T = 296\ K \end{cases}$

F. Numerical Solution

The commercial CFD code Fluent 6.3 was used to simulate airflow and temperature in the solar dryer. Unsteady airflow and heat transfer through a two-dimensional model was carried out for a typical day of August under the climatic conditions of Tlemcen (Algeria).The SIMPLE algorithm was used for pressure-velocity coupling. The iterative solution is continued until the residuals for all cells of calculation have become<10−5 for all dependent variables. A grid independence test analysis showed that the mesh grid (25938) is good enough for the studied geometry. Fig. 3 shows the validation of the present 2D CFD model by using the theoretical and experimental works of Jyotirmay Mathur et al [13]. The obtained results are in good agreement with those presented in Jyotirmay et al (2006).

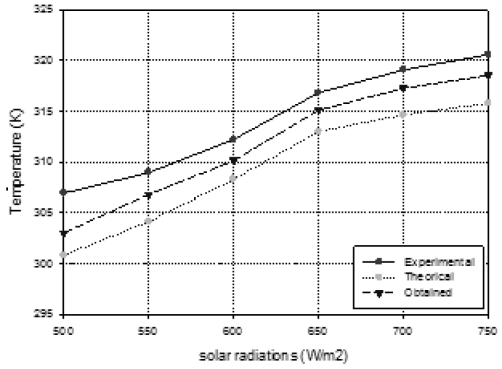

Fig. 3: Validation of the present work with those of JyotirmayMathur et al [13].

IV. RESULTS AND DISCUSSION

A. Dynamic and thermal behavior of the solar dryer without packed bed

The solar radiations and ambient temperature, presented in Fig. 2. strongly affects the temperature and airflow inside the solar dryer. The evolution of airflow and temperature of the system follows the variations of those parameters.

Fig.4. illustrates the airflow streams (a), velocity filed (b) and temperature pattern (c) over the time. During the solar radiation such, the outside air enters to the solar dryer and flows directly to the wall in front. After heating with the absorber-1, air flows up and goes around the crop trays. It is observed that the flow in the interior divides into two parts; a part passes through the crops trays then the solar chimney, the other part returns and generates a vortex with a stagnation point at the lower part of the dryer. The plots of the velocity field show a maximum speed in the vicinity of two absorbers, at the inlet and the outlet of the drying cabinet. The air velocity inside the dryer reaches a maximum value during the afternoon (3PM). It achieves 0.20 m/s at the inlet. During this period, the average temperature in drying cabinet achieves its maximum too, 323K.

In the night, the temperature of the absorber-1 is much more below and the convective heat exchange between the absorber-1 and the airflow decreases, which leads to decrease the average temperature in the drying cabinet to 298 K at midnight. At the same instant, the granite temperature is relatively high, which ensures an extended operation of the chimney.

B. Dynamic and thermal behavior of the solar dryer with packed bed

To understand the dynamic and thermal behavior of the airflow within the dryer, velocity, temperature patterns and streamlines are shown in Fig.5. The streamlines shows the airflow entering at ground level, sweeping across the floor area before being sheared vertically by the opposing wall. The flow is then redirected vertically via the packed bed before going out through the chimney. In this case the packed bed contributes to establish the within the solar dryer. During the day, the packed bed plays the role of a protective barrier; it avoids reaching temperatures that may be the origin of the product deterioration. At the afternoon, the average temperature of the drying cabinet is 318 K. This temperature is lower comparing to the case 1. However, during off sunshine hours, the packed bed releases the heat stored and assures a hot air during these hours. The average temperature of drying cabinet achieves 311 K at midnight. In average, it is 13°C higher than the previous case.

C. Effect of thickness of packed bed on the crops temperature

To produce a high quality and cost effective product the drying time must be as short as possible without using excessive heat that causes product degradation. In order to optimize the dimension of the packed bed, a comparison between the crops temperature evolution for six thickness of the packed bed (Hb = 0.05, 0.10, 0.15, 0.17, 0.20, 0.25m) is presented in Fig.6. It can be clearly seen that with a packed bed of thickness Hb=0.05 m, the temperature of the crops is maximum 323 K during the solar radiation, the maximum crops temperature decreases with the increase of the packed bed thickness. Out of these hours, the minimum crops temperature increases with the increase of the packed bed thickness. Out of these hours, the minimum crops temperature increases with the increase of the packed bed thickness.

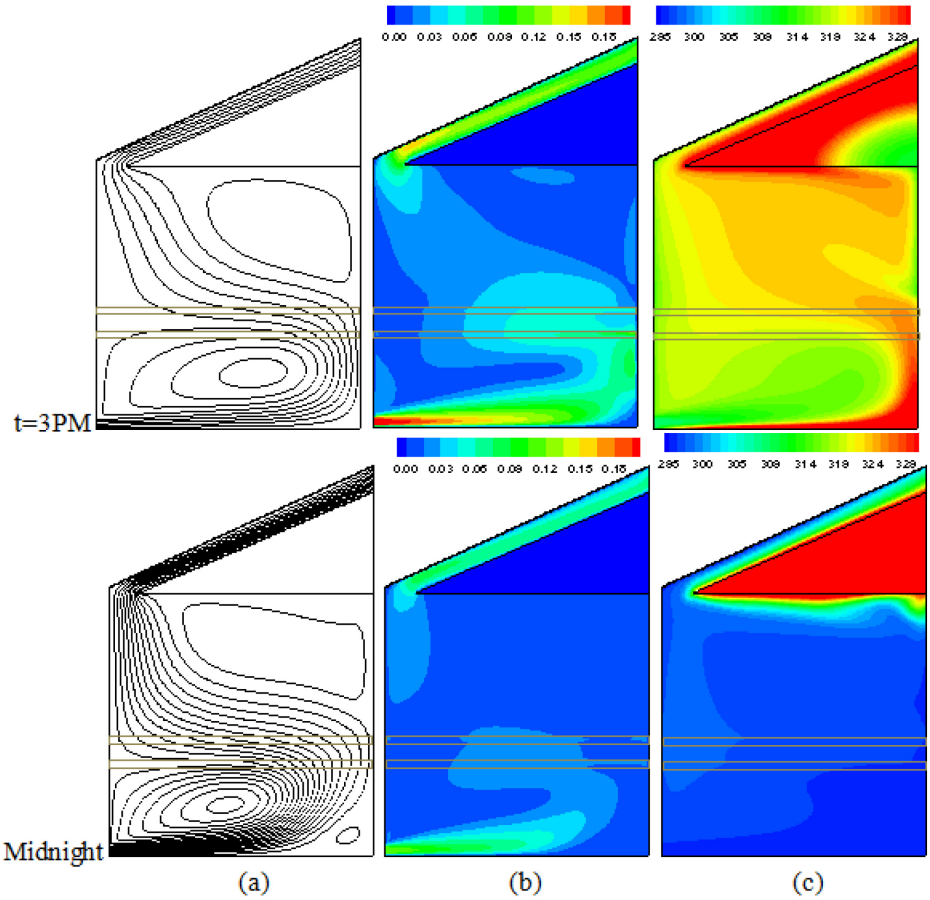

Fig.4. Contours of (a) Stream lines, (b) Velocity magnitude, (c) Temperature within the solar dryer without packed bed for two different times.

Low thickness bed provides a low thermal heat storage effect. In fact, a packed bed with greater thickness stores more thermal energy. For a thickness of 0.17 m and 0.20 m the crops temperature achieves respectively 317K and 315K as maximum and reduce during the night to 303K and 304K respectively. On the other hand, the effect of increase in thickness is decreased the fluctuation of temperature of crops between sunshine and off sunshine hours. A higher value of packed bed (between 0.10 and 0.20 m) promotes better heat storage and low peak temperature variation. From the experience, the suitable temperature of drying figs is between 317K and 323K. Drying them at a higher temperature would result in cooked figs (Trivittayasil et al. 2014)[14]. From the results, the thickness between 0.17m to 0.20m provides the suitable temperature of drying figs, because it provides a good temperature and good storage in the same time.

However above this thickness, there is a risk of producing an opposite effect and the bed does not ensure the desired temperatures. For this solar drying study, a thickness of 0.17m could be taken as appropriate

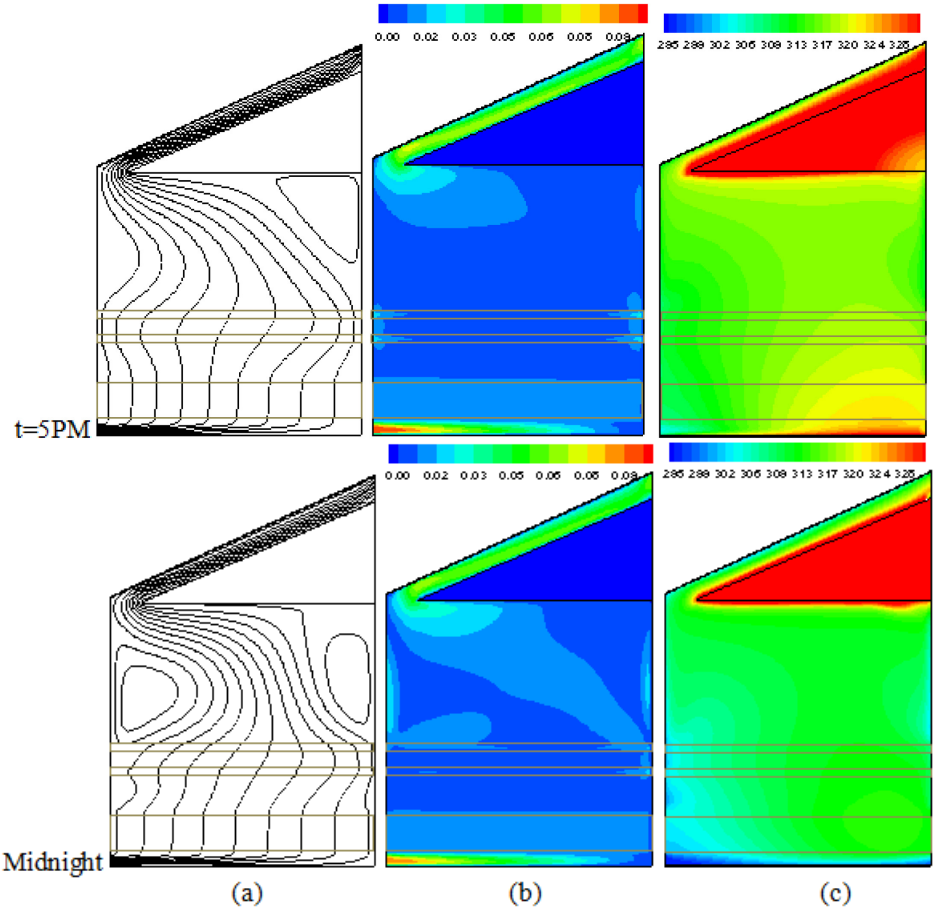

Fig.5. Contours of: (a) stream line, (b) velocity magnitude, (c) Temperature within the solar dryer with packed bed for two different times.

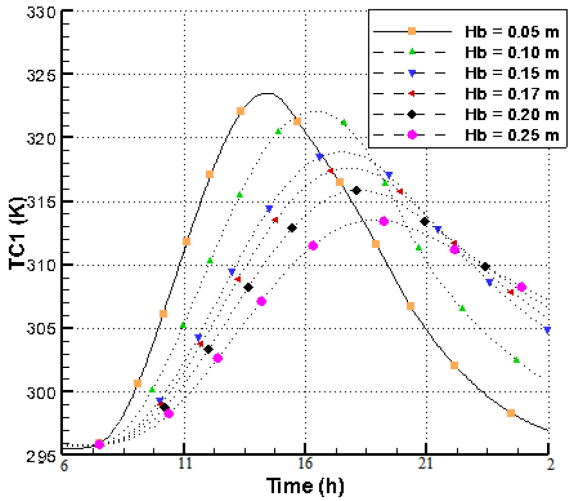

Fig. 6. Crops temperature historyT_{c1} for different thickness of packed bed at position x=0.5m, y= 0.35m.

CONCLUSION

A numerical study is proposed to simulate airflow and temperature in the solar dryer. Unsteady turbulent airflow and heat transfer through a two-dimensional model was carried out for a typical day of August under the climatic conditions of Tlemcen (Algeria). Following specific conclusions are drawn :

- During the day, the packed bed plays the role of a protective barrier; it avoids reaching temperatures that may be the origin of the product deterioration.
- The drying of the product in the trays is provided in the non sunny hours through the thermal bed which provides warm air. Variation in bed thickness directly affects the temperature of the crops.

- Increasing of the height of packed bed leads to decrease the maximum temperature during sunshine hours and ensure more stabilization of crops temperature during off sunshine hours.
- The minimum crops temperature (T_{c1}) during nighttime varied between 34°C and 35°C for a packed bed of thickness between 0.17 m and 0.2 m. In average, it was 12.5°C higher than the ambient temperature.

REFERENCES

[1] Inci Turk Togrul, DursunPehlivan,: Modelling of thin layer drying kinetics of some fruits under open-air sun drying process. Journal of Food Engineering 65 (2004) 413–425. 2004

[2] Jain, D., Tiwari, G.N., 2003. Thermal aspects of open sun drying of various crops. Journal of Energy 28, 37–54.

[3] Belessiotis, V., Delyannis, E. Drying: methods and systems – principles of drying procedures. Book n Greek. Sideris Publishing Co., Athens, p. 844. 2009

[4] Singh, P.P., Singh, S., Dhaliwal, S.S.,. Multi-shelf domestic solar dryer. Energy Conversion and Management 47, 1799–1815. 2006.

[5] P. Gbaha, H. YobouetAndoh, J. KouassiSaraka, B. Kame´nanKoua, S. Toure, Experimental investigation of a solar dryer with natural convective heat flow. Renewable Energy 32 (2007) 1817–1829. 2007

[6] El-Sebaii, A.A., Aboul-Enein, S., Ramadan, M.R.I., El-Gohary, H.G. Experimental investigation of an indirect type natural convection solar dryer. Energy Conversion and Management 43 (16), 2251–2266. 2002.

[7] Ahmed Abed Gatea,. Performance evaluation of a mixed-mode solar dryer for evaporating moisture in beans. Journal of Agricultural Biotechnology and Sustainable Development Vol. 3(4) pp. 65-71, 2011

[8] Lalit M. Bal, Santosh Satya, S.N. NaikSolar, Dryer with thermal energy storage systems for Drying agricultural food products: Review. Renewable and Sustainable Energy Reviews 14 2298–2314.

[9] Jain D. (2007) Modeling the performance of the reversed absorber with packed bed thermal storage natural convection solar crop dryer. Food Engineering;78:637–47.

[10] Amanlou Y., Zomorodian A. (2010) Applying CFD for designing a new fruit cabinet dryer. Food Engineering 101: 8–15.

[11] Bradshaw, R. D., & Myers, J. E. (1963). Heat and mass transfer in fixedand fluidized beds of large particles. ALCHE Journal, 9(5), 590–595.

[12] Swinbank, W.C. (1963) Long-wave radiation from clear skies. Quarterly Journal of the Royal Meteorological Society 9 (381), 339–348.

[13] Jyotirmay M., Sanjay M., Anupma. (2006) Summer performance of inclined roof solar chimney for natural ventilation. Energy and Buildings 38: 1156–1163.

[14] Trivittayasil V., Tanaka F., Hamanaka D., Uchino T. (2014) Prediction of surface temperature of figs during infrared heating and its effect on the quality. Biosystems Engineering 122:16- 22.

V. NOMENCLATURE

Latin letters

A_t	mirror surface, m^2
C	inertial resistance factor
C_1	constant for the turbulence model
C_2	constant for the turbulence model
C	specific heat at constant pressure, J $kg^{-1}K^{-1}$
c_μ	constant for the turbulence model
D_p	particle diameter
d	air outlet , m
e	air inlet, m
G_{sun}	solar irradiations, $W.m^{-2}$
G_k	turbulence model coefficient
g	gravitational acceleration, $m.s^{-2}$
h_0	convective heat transfer coefficient due to wind, $W.m^{-2}.K^{-1}$
H_b	height of packed bed,m
K	thermal conductivity, $W.m^{-1}.K^{-1}$
k	turbulence kinetic energy
n	normal coordinate, m
p	pression, Pa
pa	atmospheric pressure, Pa
Pr	Prandtl number
R	universal gas constant, J K^{-1} mo^{-1}
S	source term
T	temperature,°C, K
v_j	velocity magnitude y direction, $m.s^{-1}$
v_a	air velocity, $m.s^{-1}$
V_v	wind velocity; m/s
x	horizontal coordinate, m
y	vertical coordinate, m

Greek symbols

α	coefficient of absorbtion
β	coefficient of thermal expansion
ε	dissipation rate of turbulence energy ($m^2.s$)
τ	transmitivity of glass cover
ρ	density, $kg.m^{-3}$
ρ'	coefficient of reflectivity of mirrors
μ_t	turbulent dynamic viscosity ,kg (m s)-1
μ	dynamic viscosity, kg (m s)-1
σ	coefficient du rayonnement
σ_t	constant for the turbulence model
σ_k	constant for the turbulence model
σ_ε	constant for the turbulence model
ϵ	porosity
θ	coefficient of permeability
τ	coefficient of transmissivity

Subscripts

a	ambient
a_1	absorber-1
a_2	absorber-2
c_1	crops in tray-1
c_2	crops in tray-2
eff	effective
f	fluid phase in packed bed
g	glass cover
m	average
ref	reference
s	solid phase in packed bed
w	wood